Mechanistic examination of the titania photocatalyzed oxidation of ethanolamines

Satoshi Horikoshi,[a] Natsuko Watanabe,[a] Miki Mukae,[a] Hisao Hidaka*[a] and Nick Serpone[b]

[a] *Frontier Research Center for the Global Environment Protection (EPFC), Meisei University, 2-1-1 Hodokubo, Hino-shi, Tokyo, 191-8506, Japan. E-mail: hidaka@epfc.meisei-u.ac.jp*

[b] *Department of Chemistry and Biochemistry, Concordia University, 1455 de Maisonneuve Blvd. West, Montréal, Québec, H3G-1M8, Canada*

Received (in Strasbourg, France) 5th March 2001, Accepted 7th May 2001
First published as an Advance Article on the web 2nd July 2001

In this study we focus on elucidating the mechanism of the photocatalyzed transformation of the primary, secondary and tertiary amines found in ethanolamine, diethanolamine and triethanolamine when present in illuminated aqueous titania dispersions. Photodecomposition of these ethanolamines leads to the evolution of CO_2 through prior formation of various intermediate species. Ammonium (NH_4^+) and nitrate ions (NO_3^-) are the ultimate products formed in the photoconversion of the amine nitrogen atoms, with NH_4^+ cations produced in greater quantity than NO_3^- anions for all three ethanolamines. Photooxidation of triethanolamine yields various intermediates, including a 3-pyrrolidone derivative, diethanolamine, and then ethanolamine, before complete mineralization occurs. The nature of the initial steps in the photodegradation was predicted by computer-aided molecular orbital (MO) calculations of point charges, and by frontier electron densities of all atoms in the ethanolamine structures.

Water-soluble organic pollutants continue their incessant damage on aquatic ecosystems despite global discussions taking place in many countries on exploring ways to arrest environmental damage. A conclusive and workable technology that can safely dispose of a broad spectrum of products by means other than conventional incineration and internment is still lacking. Ethanolamine (EA) is an industrial product extensively used in cosmetics, as a plasticizer in polymers, in paints, and in a variety of other applications. Discharge of ethanolamines into waterways and the atmosphere occurs without regulatory oversight. When present in ecosystems, they can cause considerable damage to animals and humans owing to their carcinogenic nature and suspected endocrine disruptor qualities.

A nitrogen-containing substance can be mineralized photocatalytically to NH_4^+ cations and NO_3^- anions; concurrently, the carbon atoms are mineralized to CO_2 through a number of oxidative hydroxylated intermediates, and through carboxylic acids such as the acetic and formic acids.[1,2] Despite the few reports on the photooxidative degradation of nitrogen-bearing compounds,[3–9] details of the degradative pathways remain unresolved in many cases as they relate to the NH_4^+/NO_3^- ion ratios or to the identity of the oxidized intermediates.

The present study focuses on three fundamental aspects in the overall photocatalyzed transformation of ethanolamines, namely: (a) the initial steps in the photooxidative process taking place on the TiO_2 surface, (b) the photoconversion pathways of primary, secondary and tertiary amines in aqueous TiO_2 dispersions, and (c) the overall photomineralization process. Conversion of the nitrogen atoms in the three amines was examined from various viewpoints, namely (1) formation of NH_4^+ and NO_3^- ions, (2) disappearance and/or appearance of a primary amine, (3) formation of carboxylic acids, (4) generation of intermediates that might display useful UV absorption features, (5) detection of intermediates by liquid chromatographic mass spectrometric (LC/MS) methods, (6) evolution of carbon dioxide, and (7) simulation of various characteristics of the pathway(s) by frontier electron density and point charge MOPAC calculations, as these pertain to adsorption of ethanolamines on the TiO_2 particle surface and to attack by the photogenerated $^{\bullet}OH$ radicals. A degradation mechanism is inferred on the basis of experimental results and theoretical considerations.

Experimental

Ethanolamine (EA: $NH_2CH_2CH_2OH$), diethanolamine [di-EA: $NH(CH_2CH_2OH)_2$] and triethanolamine [tri-EA: $N(CH_2CH_2OH)_3$] were supplied by Wako Pure Chemicals Co. Ltd. Titanium dioxide was Degussa P-25 (particle size, 20–30 nm by TEM observation; 83% anatase and 17% rutile as determined by X-ray diffraction; surface area, 53 $m^2\ g^{-1}$ by BET methods). Aqueous dispersions (50 mL) consisting of 100 mg TiO_2 particles and the appropriate substrate (0.1 mM) were contained in a 124 mL Pyrex reactor (headspace volume *ca.* 74 ml). The mixture was ultrasonicated for 5 min and maintained under continuous agitation during illumination with a 75 watt Hg lamp with a power density of *ca.* 2.7 mW cm^{-2} in the wavelength range 310 to 400 nm (maximum emission, $\lambda = 365$ nm). The dispersion was purged with oxygen gas for *ca.* 15 min prior to irradiation. The temporal evolution of CO_2 was monitored by gas chromatography using an Ookura Riken chromatograph (model 802; TCD detector) and a Porapack Q (for CO_2 gas) column; helium was the carrier gas. The concentrations of photogenerated NH_4^+ and NO_3^- ions were assayed employing a JASCO HPLC chromatograph equipped with a CD-5 conductivity detector, using either a Y-521 cationic column or an I-524 anionic column.

Spectrofluorometric quantitation of the primary amine was carried out using a common procedure. After a given UV irradiation period, the degraded solution was mixed in 0.15 mL of a borate buffered solution (pH = 9), followed by addition of an acetone solution (0.15 mL) of fluorescamine (0.03%). The resulting solution was analyzed with a JASCO FP-770 spectrofluorometer. The intermediates produced from the

photodegradation of the ethanolamines were identified using an Agilent Technologies HP1100 series LC/MS (liquid chromatography/negative and positive electrospray mass spectra) apparatus in a mixed eluent of methanol–water (1 : 1 by volume). The LC/MS system was equipped with an Agilent Eclipse XDB-C_8 column.

Computer simulations were performed using the CAChe Worksystem version 3.2 package (Fujitsu, 1999) implemented on an Intel P-III and Windows 2000 system. The frontier electron densities used to assess the positions of $^{\cdot}OH$ radical attack and the point charges of all the atoms in the ethanolamines were calculated by a MOPAC/PM3[10] wavefunction for each specimen at a geometry determined by performing a pre-optimization calculation in Molecular Mechanics using Augmented MM3. This was followed by optimization of the geometry calculations using MOPAC and PM3 parameters, which also included solvation effects that were simulated by COSMO.

Results and discussion

Photooxidation of ethanolamines

TiO_2 particles absorb UV light of energy greater than the bandgap (*ca.* 3.2 eV) to generate electron/hole pairs [eqn. (1)]. Following various steps, the holes (h^+) are ultimately trapped by HO^- ions or by H_2O at the particle surface to yield H^+ and $^{\cdot}OH$ radicals [eqn. (2)]. Our data do not preclude the possibility of direct hole scavenging by the base to form cation radicals; however, under our conditions, this scenario is rather unlikely. Concomitantly, dioxygen molecules react with electrons (e^-) in the conduction band to yield superoxide radical anions, $O_2^{\cdot -}$, which on protonation generate the hydroperoxy, $^{\cdot}OOH$, radicals [eqn. (3)].

$$TiO_2 + h\nu \xrightarrow{h\nu > E_{bg}} TiO_2(e^-_{cb} + h^+_{vb}) \rightarrow e^-_{cb} + h^+_{vb} \quad (1)$$

$$h^+ + H_2O \text{ (or } OH_{surf.}{}^-) \rightarrow {}^{\cdot}OH + H^+ \quad (2)$$

$$e^-_{cb} + O_2 \rightarrow O_2^{\cdot -} \quad (3a)$$

$$O_2^{\cdot -} + H^+ \rightarrow {}^{\cdot}OOH \quad (3b)$$

$$^{\cdot}OH \text{ (or } ^{\cdot}OOH) + EAs \rightarrow \text{Oxidative products} \quad (4)$$

The electrical charge of the TiO_2 particle surface is positive due to an excess of protons from H_2O [eqn. (2)], or from the solution if acidic. Accordingly, the negatively charged atoms in the structure of the bases will be attracted onto the surface of TiO_2 by simple Coulombic forces, and thus $^{\cdot}OH$ radicals photogenerated on the TiO_2 surface are expected to be the major oxidative agents to attack the adsorbed substrates [eqn. (4)].

The temporal evolution of NH_4^+ and NO_3^- ions produced in the course of the photodegradation of ethanolamine (EA), diethanolamine (di-EA) and triethanolamine (tri-EA) is illustrated in Fig. 1. In all cases, the overall yield of NH_4^+ ions was greater than the corresponding yield of NO_3^- ions. No evolution of N_2 gas was detected under our experimental conditions, and we infer none was produced. The ratio $[NH_4^+]/[NO_3^-]$ in the photoconversion of the amine nitrogen in EA, di-EA and tri-EA was, respectively, 6.1, 3.0 and 3.0 after 8 h irradiation. The overall conversion yield of each of the ethanolamines was about 98.5 to 100% after irradiation of the aqueous ethanolamine/TiO_2 dispersion for an 8 h period.

Results in Fig. 1 also show that formation of NO_3^- ions in the primary case (*i.e.*, in EA) was less than for the secondary and tertiary amines after the 8 h period: for EA, $[NO_3^-]$ was 0.014 mM while for di-EA and tri-EA it was 0.025 mM. Interestingly, for another system that has a chemical structure similar to ethanolamine ($NH_2CH_2CH_2OH$), namely β-alanine ($NH_2CH_2CH_2COOH$), the $[NH_4^+]/[NO_3^-]$ ratio is nearly

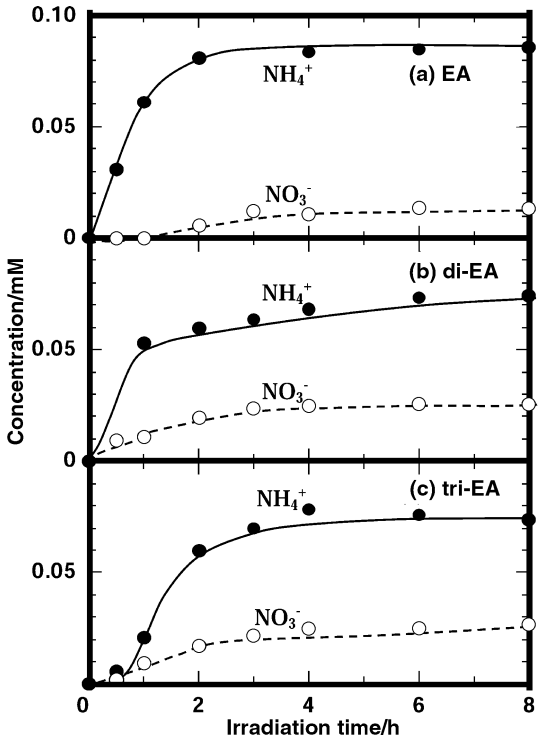

Fig. 1 Generation of NH_4^+ (●) and NO_3^- (○) ions in the photodecomposition of (a) ethanolamine, (b) diethanolamine and (c) triethanolamine under UV irradiation.

double (ratio is 12; see, for example, ref. 1). The difference between these two similar structures is the length between the amine group and the oxygen atom(s), which would presumably place the amine function in ethanolamine further away from the TiO_2 particle surface at which the primary oxidative step occurs. Also, formation of NO_3^- ions is immediate for the di-EA and tri-EA amines; for ethanolamine there is an induction period of at least 1 to 1.5 h before NO_3^- ions are detected. In contrast, formation of NH_4^+ ions in ethanolamine is prompt, whereas evolution of this cation from diethanolamine and triethanolamine occurs only after a short induction period of *ca.* 0.5 h.

The kinetics for formation of ammonium and nitrate ions, together with those for the evolution of carbon dioxide, and the yields of NH_4^+ ions, NO_3^- ions and CO_2 are summarized in Table 1. It is evident that formation of NH_4^+ ions is fastest for ethanolamine and nearly 20% slower for the di- and triethanolamine systems, after due consideration of the induction period(s) noted above. Similarly, formation of NO_3^- ions is faster for ethanolamine than for the other two substrates. In contrast, evolution of carbon dioxide is fastest and nearly identical for ethanolamine and triethanolamine; it is significantly slower for diethanolamine. Also given in Table 1 are the *lower limits* of the quantum yields (*i.e.*, photonic efficiencies) for the formation of ammonium and nitrate ions, and for carbon dioxide (photon flow was 5.3×10^{-4} einstein h^{-1}).

As noted earlier, the concentration of primary amines can be quantified using the emission intensity from the photoluminescence of the solution in the presence of fluorescamine. Degradation of diethanolamine and triethanolamine is expected to produce a primary amine on its way to mineralization. Fig. 2 illustrates the temporal behavior of all three ethanolamines in terms of the quantity of primary amine formed *vs.* irradiation time for up to 5 h. Both diethanolamine and triethanolamine decompose through formation of a primary amine function, which we infer to be ethanolamine or some equivalent species (see below).

Table 1 Kinetics for formation of NH_4^+ and NO_3^- ions and carbon dioxide CO_2 in the course of the photooxidative degradation of ethanolamine (EA), diethanolamine (di-EA) and triethanolamine (tri-EA), together with the yields after 8 h of illumination in an aqueous titania dispersion and the lower limits of the quantum yields photonic efficiencies ξ of formation of NH_4^+ and NO_3^- ions and CO_2

	Ethanolamine	Diethanolamine	Triethanolamine
$k_{NH_4^+}/h^{-1}$	1.05 ± 0.13	0.80 ± 0.14	0.88 ± 0.11
$k_{NO_3^-}/h^{-1}$	0.77 ± 0.20	0.56 ± 0.06	0.48 ± 0.04
k_{CO_2}/h^{-1}	1.22 ± 0.15	0.90 ± 0.06	1.33 ± 0.08
$[NH_4^+]$/mM	0.086	0.075	0.075
$[NO_3^-]$/mM	0.014	0.025	0.025
$[CO_2]$/mM	0.16(0.20)[a]	0.33(0.40)[a]	0.49(0.60)[a]
$[NH_4^+]/[NO_3^-]$	6.1	3.0	3.0
$\xi_{NH_4^+}$	0.20	0.15	0.17
$\xi_{NO_3^-}$	0.15	0.11	0.091
ξ_{CO_2}	0.11	0.043	0.042

[a] Expected yield of carbon dioxide for 100% photomineralization.

The fairly rapid decrease in the concentration of the primary amine substrate, ethanolamine, led to a 90% conversion yield after only 2 h of illumination of the dispersion, a time identical to that needed (Fig. 1) to produce nearly all of the NH_4^+ cations. The slower disappearance of ethanolamine after the 2 h irradiation period is attributed to the slower formation of the NO_3^- ions (Table 1). For the di-EA and tri-EA systems, their decomposition yielded the maximum amount of the primary amine function after 1 h of illumination. The primary amine produced from tri-EA rapidly degraded almost completely after 2 h; however, the concentration of the primary amine from decomposition of diethanolamine was fairly constant between the 1 and 3 h illumination period, after which it decreased fairly rapidly to yield the NH_4^+ and NO_3^- ionic species. Insofar as the kinetics of formation of the primary amine from the degradation of di-EA and tri-EA amines are concerned, the data in Fig. 2 show that di-EA converts into a primary amine faster than triethanolamine. We infer from this observation that the degradative pathway of tri-EA will be somewhat more complex than the decomposition pathway of diethanolamine.

The temporal evolution of CO_2 gas from the photomineralization of the ethanolamines is depicted in Fig. 3. The order of the quantity of CO_2 evolved was tri-EA (0.49 mmol L^{-1}) > di-EA (0.33 mmol L^{-1}) > EA (0.16 mmol L^{-1}). The photomineralization yield was nearly identical in all three cases, however: 81% for EA, 83% for di-EA and 82% for tri-EA. The extent of adsorption of the ethanolamines on the TiO_2 particle surface increased with initial concentration. The photomineralization of the carbon atoms differed from the nitrogen atom. The concentration of carbon dioxide evolved depends on the number of carbon atoms in the ethanolamine homologs. The ethyl group was converted nearly quantitatively to CO_2, irrespective of the chemical composition of the ethanolamines. Nonetheless, the results of Fig. 3 do show that about 20% of the carbon atoms are unaccounted for, suggesting that some other intermediate(s) did form, which resisted photomineralization under the conditions used.

Past experience has taught us that oxidation of the aliphatic alcohol function in the ethanolamines should lead to formation of the carboxylic acid species. Indeed, as demonstrated in the HPLC results of Fig. 4, photooxidation of diethanolamine produces acetic acid within 1 h of irradiation. Photooxidation of triethanolamine yields acetic acid and immediately thereafter produces formic acid in less than 2 h of illumination. These acids undergo further oxidation fairly rapidly as they were no longer detected beyond the respective irradiation periods. This is not too surprising since within the 2 h irradiation period, evolution of carbon dioxide had nearly reached

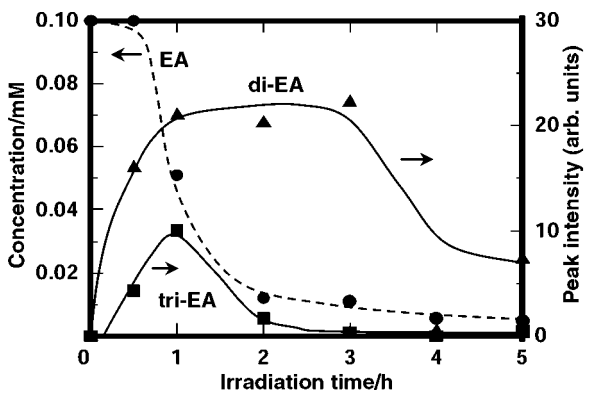

Fig. 2 (a): Disappearance and formation of primary amine in the photodegradation of ethanolamine (●), diethanolamine (▲) and triethanolamine (■).

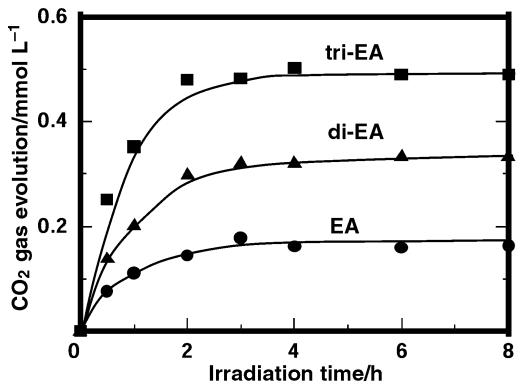

Fig. 3 Evolution of CO_2 gas during the photodegradation of ethanolamine (●), diethanolamine (▲) and triethanolamine (■).

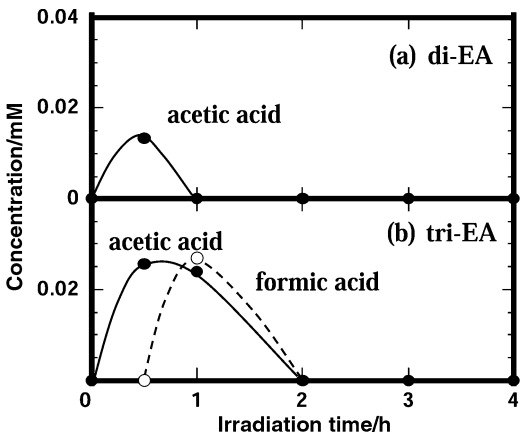

Fig. 4 Formation of formic acid (○) and acetic acid (●) during the photodegradation of (a) diethanolamine and (b) triethanolamine.

its maximal value for all three ethanolamines (see Fig. 3). The difficulty of detecting carboxylic acid functions strongly infers that evolution of CO_2 is faster than formation of the carboxylic acids.

We presume (at this stage) that the photodegradation of diethanolamine and triethanolamine, which bear two and three ethanol moieties, respectively, must involve a complex series of competitive photooxidative steps and formation of various intermediates. The overall photooxidation of the simpler ethanolamine substrate likely proceeds through a simpler mechanism. To aid in our understanding of the initial photooxidative steps, we carried out theoretical calculations (see Experimental) the results of which we now describe below.

Theoretical calculations

The calculations were carried out using molecular orbital methods (see Experimental for further details) to assess the point charges and the frontier electron density on each atom of the ethanolamine substrates.[11] The results are summarized in Tables 2–4 for ethanolamine, diethanolamine and triethanolamine, respectively. Determining which atom(s) carries the largest negative point charge provides clues as to the direction of approach of the ethanolamine and to the ultimate point of adsorption of the ethanolamines onto the positively charged TiO_2 particle surface in acidic aqueous media (pH below 6.3). To the extent that the oxygen atoms in the alcoholic function, –OH, are the most negatively charged atoms, they are inferred to be the major point of contact between the positively charged TiO_2 surface and the ethanolamines. In this regard, the ease of adsorption on a positively charged TiO_2 surface is expected to be in the order tri-EA > di-EA > EA in a ratio of 3 : 2 : 1.

Table 2 Calculated point charges and frontier electron densities for all atoms in ethanolamine

$N^1H_2-C^2H_2-C^3H_2-O^4H$

Atom	Partial charge	Frontier electron density
N^1	−0.109	0.953
C^2	−0.125	0.282
C^3	0.074	0.180
O^4	−0.404	0.096
H^5	0.053	0.105
H^6	0.058	0.127
H^7	0.065	0.042
H^8	0.055	0.105
H^9	0.042	0.031
H^{10}	0.043	0.036
H^{11}	0.246	0.043

Table 3 Calculated point charges and frontier electron densities for all atoms in diethanolamine

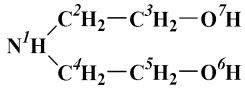

Atom	Partial charge	Frontier electron density
N^1	−0.114	0.934
C^2	−0.118	0.216
C^3	0.076	0.088
C^4	−0.119	0.217
C^5	0.077	0.089
O^6	−0.403	0.047
O^7	−0.403	0.047
H^8	0.074	0.101
H^9	0.070	0.025
H^{10}	0.058	0.064
H^{11}	0.044	0.010
H^{12}	0.045	0.013
H^{13}	0.058	0.064
H^{14}	0.070	0.024
H^{15}	0.045	0.013
H^{16}	0.044	0.010
H^{17}	0.247	0.019
H^{18}	0.247	0.019

Table 4 Calculated point charges and frontier electron densities for all atoms in triethanolamine

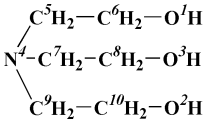

Atom	Partial charge	Frontier electron density
O^1	−0.404	0.028
O^2	−0.402	0.028
O^3	−0.403	0.030
N^4	−0.089	0.943
C^5	−0.118	0.172
C^6	0.065	0.059
C^7	−0.112	0.186
C^8	0.065	0.064
C^9	−0.111	0.197
C^{10}	0.068	0.058
H^{11}	0.248	0.010
H^{12}	0.248	0.011
H^{13}	0.247	0.011
H^{14}	0.080	0.008
H^{15}	0.061	0.041
H^{16}	0.051	0.007
H^{17}	0.045	0.007
H^{18}	0.059	0.043
H^{19}	0.074	0.009
H^{20}	0.047	0.007
H^{21}	0.051	0.007
H^{22}	0.073	0.014
H^{23}	0.060	0.049
H^{24}	0.052	0.005
H^{25}	0.045	0.008

The predominant oxidizing entity in photooxidations that involve TiO_2 particulates are the surface-bound $^{\cdot}OH$ radicals produced by reaction of valence band holes with the ubiquitous OH^- groups and water molecules located on the surface of the particles, as determined from several earlier studies in our laboratories[11] and the many reports in the literature. The atomic position for attack of the ethanolamines by these $^{\cdot}OH$ radicals can be predicted from the calculated frontier electron densities. The data in Tables 2–4 show that the nitrogen atoms of the three ethanolamines are the positions of richest frontier electron density. We suggest that the ethanolamines chemisorb dissociatively through the alcoholic function, and that the preferred points of attack by the $^{\cdot}OH$ radicals are, in principle, the nitrogen atoms if these are close to the particle surface where redox chemistry occurs. It is relevant to note that these $^{\cdot}OH$ radicals are formed at and remain on the surface. Before proceeding with a more detailed discussion of the photooxidation pathways, it is worthwhile to examine additional data on the nature of the intermediates formed in the photodegradation process that will be germane to a more comprehensive view of the complexity of events that take place.

Electrospray mass spectral detection of intermediates

Detection of intermediates produced during the photodegradation of the ethanolamines was carried out by LC/MS spectrometric techniques. Several intermediates were produced, as evidenced in Fig. 5 for triethanolamine for example (see below), in less than 90 min of irradiation. The photooxidation

mechanism is inferred from the characteristic mass spectral peaks for all three ethanolamines obtained at various UV irradiation times. Typical intermediates were identified from both positive {*i.e.*, cationic compounds: [species + H^+]} and negative {*i.e.*, anionic compounds: [species − H^+]} modes.

Ethanolamine. The initial peak seen at a mass/charge ratio (*m/z*) of 62.1 corresponds to the cationic species [EA + H^+] for ethanolamine (molecular mass 61.1 g mol^{-1}), and for which no signal was detected after 20 min of UV illumination. After only 5 min of irradiation, peaks at *m/z* 60.1 (positive mode) and 74.1 (negative mode) were evident. We assign these to the chemical structures NH_2CH_2CHO or CH_3COOH and NH_2CH_2COOH, respectively. However, to the extent that no CH_3COOH was detected by HPLC methods for ethanolamine (see Fig. 4), we conclude that the *m/z* 60.1 signal is due to the aminoacetaldehyde NH_2CH_2CHO. Signals at *m/z* 63.1 and 61.1 (positive data) are also observed during the first 2 h of UV illumination; they are due to ethylene glycol $HOCH_2CH_2OH$ and the hydroxyacetaldehyde $HOCH_2CHO$, respectively.

Diethanolamine. Inferences on the photooxidative pathway for diethanolamine are made on the basis of the intermediates indicated by the LC/MS analysis for positive electrospray mode (cationic species). Within the first 30 min of UV illumination of the diethanolamine/TiO_2 dispersion a signal for diethanolamine was observed at *m/z* 106.1: [di-EA + H^+]. After only 5 min of irradiation three new signals emerged in the mass spectra at *m/z* 86.1, 104.1 and 118.1, which we assign to 3-pyrrolidone (NC_4H_7O), $HOCH_2CH_2NHCH_2CHO$ and to $(O)CHCH_2NHCH_2COOH$ and/or $(O)CHNHCH_2CH_2COOH$, respectively.

The MS spectra of anionic compounds (*i.e.*, negative mode) show formation of an intermediate after 10 min of irradiation whose signature appears at *m/z* 118.1. We identify this species as $HOCH_2CH_2NHCH_2COOH$. Intermediates formed from the degradation of diethanolamine undergo further photooxidation under the conditions used to generate smaller species such as ethanolamine $NH_2CH_2CH_2OH$, seen at *m/z* 62.1.

Triethanolamine. The complexity of the mass spectral results from the photodegradation of the ethanolamines is exemplified by the LC/MS spectra for triethanolamine illustrated in Fig. 5 for cationic species (positive mode). The signal corresponding to triethanolamine was observed initially at *m/z* 150.1. After 5 min of UV illumination, however, the tri-EA signature totally disappeared, but new peaks appeared at *m/z* 130.1 and 148.1.

These are assigned to *N*-(2-hydroxyethyl)pyrrolidone [$HOCH_2CH_2N(C_4H_6O)$] and to $(O)CHCH_2N(CH_2CH_2OH)_2$, respectively. The MS spectral pattern seen after 30 min of irradiation displays a signal at *m/z* 106.1, which is the signature of diethanolamine produced from the breakdown of triethanolamine. After 90 min of illumination the mass spectral results show a signal at *m/z* 62.1 that we attribute to ethanolamine formed from further degradation of the diethanolamine intermediate.

As evidenced earlier, photooxidation of the hydroxyethyl functions ($-CH_2CH_2OH$) takes place concomitantly with formation of unusual intermediates and ultimately leads to the evolution of carbon dioxide. The many other peaks observed in the LC/MS spectra are other unidentified amines, aldehydes and carboxyl-type derivatives.

UV spectral detection of intermediates

Formation of intermediates in the photooxidation of diethanolamine and triethanolamine was also monitored by UV absorption spectroscopy (Fig. 6). The new UV absorption features are attributed to formation of 3-pyrrolidone and/or related 3-pyrrolidone derivatives. Initially, diethanolamine and triethanolamine (0.1 mM solution) exhibited a single band around 192 nm (absorbance = 0.143 and 0.156, respectively). UV illumination led to an increase in the absorption band (absorbance = 0.237 and 0.300) after 15 min of irradiation and to a very slight red-shift of the band to 193 nm. The spectral intensity decreased on further irradiation. A small new peak at 290 nm was observed [inset to Fig. 6(a)] for diethanolamine and at 335 nm for triethanolamine [inset to Fig. 6(b)]. The intermediates responsible for these two new UV absorption bands correspond to those whose signatures in the LC/MS spectra appear at *m/z* 86.1 (diethanolamine LC/MS spectra) and at *m/z* 130.1 (triethanolamine LC/MS spectra). The weak UV absorption at 294 nm in a mixed solution of 3-pyrrolidone and diethanolamine (each 0.1 mM) corresponds closely to the new band in the inset to Fig. 6(a). Consequently,

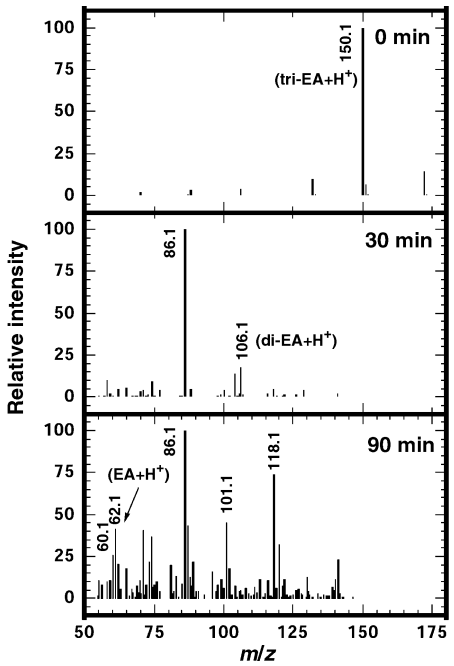

Fig. 5 Mass spectral signals during the photooxidation of triethanolamine after UV irradiation times of 0, 30 and 90 min.

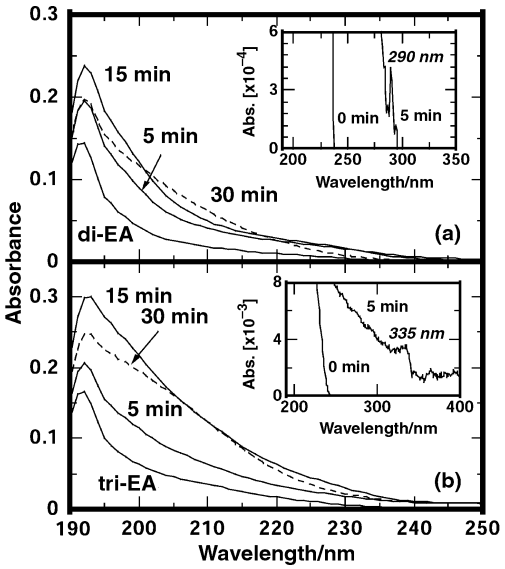

Fig. 6 Temporal UV spectral patterns for the generation of intermediates in the photodecomposition of (a) diethanolamine and (b) triethanolamine. The insets show a magnification of the appropriate wavelength range.

we describe the increase of the UV absorption bands with irradiation time as arising from the formation of 3-pyrrolidone or to some related derivative.

Photodegradation mechanisms

Ethanolamine. The data presented above point to a tentative mechanism in the photodegradation of ethanolamine suggested in Scheme 1 (note that species in brackets were not detected under our experimental conditions). We view the first step in the process as dissociative chemisorption of the ethanolamine through the –OH oxygen atoms onto the positively charged TiO_2 particle surface. On irradiation and subsequent formation of $^{\bullet}OH$ radicals, the ethanolamine is poised to undergo transformation through a series of sequential and competitive events. These will involve attack at the C^2 and C^3 carbon atoms and the N atom by the $^{\bullet}OH$ species through steps a, c and b, respectively. Step a yields a C^2-radical intermediate that on further interaction with $^{\bullet}OH$ radicals and the acidic medium ultimately leads to ethylene glycol, $HOCH_2CH_2OH$, and NH_4^+ ions. Continued oxidation of the glycol yields $HOCH_2CHO$ and in due course carbon dioxide. Interaction of surface-adsorbed $^{\bullet}OH$ species with the C^3 carbon in step c leads to formation of the acetamide H_2NCH_2CHO and subsequently the amino acid H_2NCH_2COOH, which on further interaction with the $^{\bullet}OH$ radicals yields formamide (undetected) and ultimately carbon dioxide, nitrate and ammonium ions. Step b illustrates the fate of the chemisorbed ethanolamine when the $^{\bullet}OH$ radical attacks the amine N atom of ethanolamine, which then undergoes other degradation steps to produce ethylene glycol, ammonium ions and nitrate ions. We do not preclude formation of a peroxy amine derivative generated as an oxidative intermediate species by attack on the amine moiety by $^{\bullet}OOH$ radicals. Thus, the existence of hydroperoxy cation radicals such as $HOCH_2CH_2N^+{}^{\bullet}H_2OOH$ are possible intermediate oxidative species.

Diethanolamine. The theoretical calculations and the experimentally detected species produced in the photoconversion of diethanolamine during irradiation of the TiO_2 dispersion suggest the simplified mechanism proposed in Scheme 2. The diethanolamine is also dissociatively chemisorbed on the TiO_2 particle through both oxygen atoms of the –OH groups. Because the diethanolamine structure is now held on the surface (see Scheme 2) in a manner that places the amine function away from the surface, and because the $^{\bullet}OH$ radicals are surface bound, it is unlikely that the latter species will significantly interact with the amine nitrogen even though this atom bears the largest frontier electron density (see Table 3). Consequently, the $^{\bullet}OH$ radicals will preferentially attack the carbon atom closest to the particle surface, namely the C^3 carbon atom (see Table 3) to yield first the hydroxyethyl acetamide

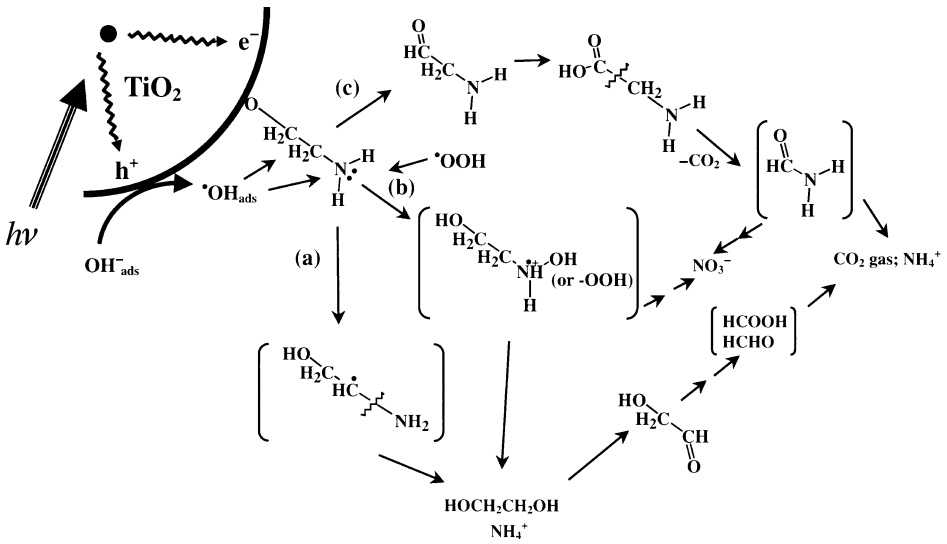

Scheme 1

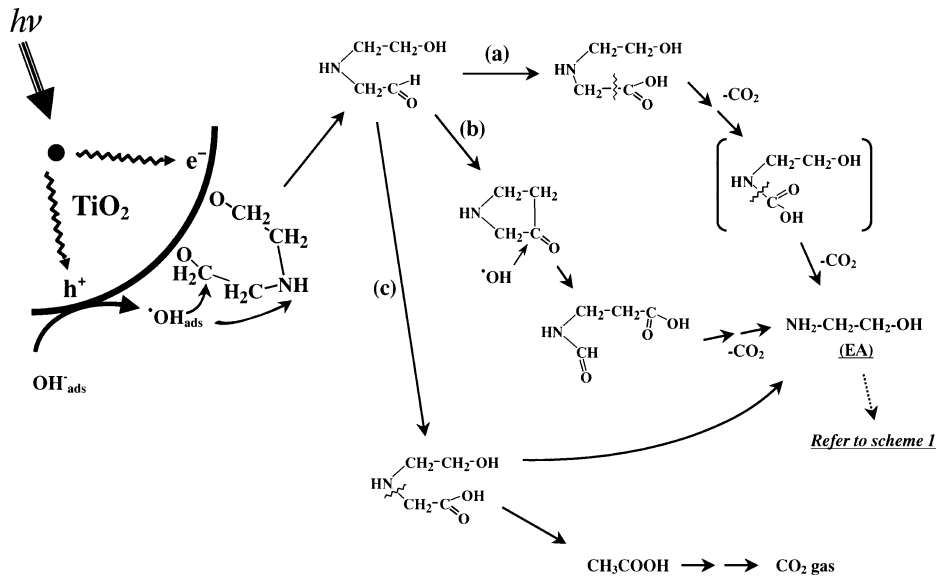

Scheme 2

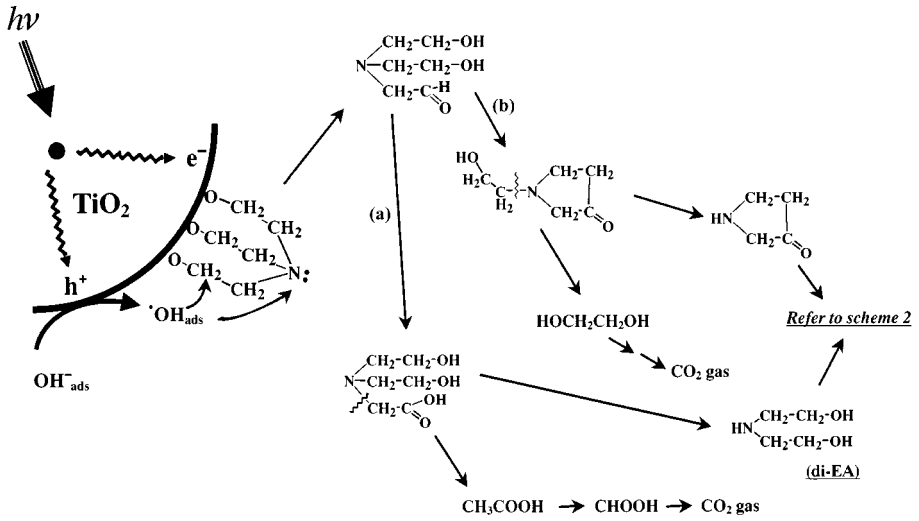

Scheme 3

intermediate $HOCH_2CH_2NHCH_2CHO$. Further oxidation of this species yields the 3-pyrrolidone intermediate formed through an aldol condensation event (step b), and the hydroxyethyl amino acid $HOCH_2CH_2NHCH_2COOH$ through steps a and c. Cleavage of the C^2–N bond in this amino acid yields acetic acid and ethanolamine, whereas rupture of the C^4–C^5 bond through further oxidation leads to loss of CO_2 and to the (undetected) intermediate $HOCH_2CH_2NHCOOH$. Subsequent loss of carbon dioxide from this latter intermediate through oxidation of the –NHCOOH fragment leads to another molecule of ethanolamine.

As expected from the rich frontier electron density in the 3-pyrrolidone derivative, opening of the ring at the C^3=O carbon atom through attack by ·OH radicals yields the $(O)CHNHCH_2CH_2COOH$ intermediate. Loss of CO_2 through continued oxidation also yields ethanolamine. Photodegradation of this ethanolamine, as in Scheme 1, yields additional carbon dioxide and evolution of NH_4^+ and NO_3^- ions in the order $NH_4^+ \gg NO_3^-$.

Triethanolamine. The mechanism for the photodecomposition of triethanolamine is illustrated in Scheme 3. Dissociative chemisorption now occurs through all three oxygen atoms of the –OH groups in the amine. Here, the triethanolamine structure is rigidly held on the TiO_2 particle surface, even more so than in diethanolamine, such that the amine nitrogen atom is held away from the surface, rendering difficult any interaction between the surface-bound ·OH radicals and the amine nitrogen atom.

Initially, attack of the ·OH radical onto the carbon atom closest to the surface (*e.g.*, C^6, see Table 4) leads to formation of the aldehyde intermediate $(HOCH_2CH_2)_2NCH_2CHO$, seen at *m*/*z* 148.1 (not shown in Fig. 5) within the first 15 min of UV irradiation of the titania suspension. After 30 min of illumination, this intermediate is completely converted to the acid form $(HOCH_2CH_2)_2NCH_2COOH$ (step a in Scheme 3) and to the N-substituted 3-pyrrolidone $HOCH_2CH_2N(C_4H_6O)$ species seen prominently at *m*/*z* 130.1 after 5 min of irradiation, and formed by an aldol condensation step. On further illumination, the carboxylic acid intermediate undergoes scission of the C^5–N bond to produce diethanolamine and acetic acid, the latter undergoing further oxidation to formic acid and carbon dioxide. Scission of the C–N bond in the $HOCH_2CH_2N$ group of the 3-pyrrolidone derivative yields ethylene glycol and the unsubstituted 3-pyrrolidone species (NC_4H_7O), which displays a prominent signal at *m*/*z* 86.1 after 30 min of irradiation. This 3-pyrrolidone derivative subsequently undergoes further oxidation as indicated in Scheme 2. The diethanolamine and subsequently the ethanolamine produced undergo further degradation as per Schemes 2 and 1, respectively, to ultimately produce the mineralization products: carbon dioxide, and ammonium and nitrate ions.

Concluding remarks

We have examined the photomineralization of three ethanolamines and have unraveled some of the steps that occur during the processes. We have also identified by electrospray mass spectral methods and other techniques some of the intermediate species produced, the most notable of which is the 3-pyrrolidone system. From these data, we have inferred an overall mechanism embodied by Schemes 1–3, albeit it must be recognized that the photooxidative pathway is only a working hypothesis.

Acknowledgements

We are grateful to the Japanese Ministry of Education, Culture, Sports, Science and Technology of Japan (Grant-in-Aid for Scientific Research (c) no. 10640569 to H. H.) and to the Natural Sciences and Engineering Research Council of Canada (Ottawa; grant no. A5443 to N. S.) for generous support of our work.

References

1 K.-C. Low, S. R. McEvoy and R. W. Matthews, *Environ. Sci. Technol.*, 1991, **25**, 460.
2 G. K.-C. Low, S. R. McEvoy and R. W. Matthews, *Chemosphere*, 1989, **19**, 1611.
3 E. Pelizzetti, C. Minero, P. Piccinini and M. Vincenti, *Coord. Chem. Rev.*, 1993, **125**, 183.
4 C. Maillard, C. Guillard and P. Pichat, *Chemosphere*, 1992, **24**, 1085.
5 C. Maillard, C. Guillard and P. Pichat, *New J. Chem.*, 1994, **18**, 941.
6 K. Nohara, H. Hidaka, E. Pelizzetti and N. Serpone, *J. Photochem. Photobiol. A: Chem.*, 1997, **102**, 265.
7 S. Horikoshi, N. Serpone, J. Zhao and H. Hidaka, *J. Photochem. Photobiol. A: Chem.*, 1998, **118**, 123.
8 S. Horikoshi, N. Serpone, S. Yoshizawa, J. Knowland and H. Hidaka, *J. Photochem. Photobiol. A: Chem.*, 1998, **120**, 63.
9 D. S. Muggli, J. T. McCue and J. L. Falconer, *J. Catal.*, 1998, **173**, 470.
10 M. J. S. Dewar and W. Thiol, *J. Am. Chem. Soc.*, 1977, **99**, 4899; J. P. Stewart, *J. Comput. Chem.*, 1989, **10**, 209.
11 H. Hidaka, S. Horikoshi, K. Ajisaka, J. Zhao and N. Serpone, *J. Photochem. Photobiol. A: Chem.*, 1997, **108**, 197.